*Physics of the Solid State, Vol. 42, No. 2, 2000, pp. 356–363. Translated from Fizika Tverdogo Tela, Vol. 42, No. 2, 2000, pp. 347–353.*


## LOW-DIMENSIONAL SYSTEMS AND SURFACE PHYSICS

# Thermodesorption of Silicon from Textured Tantalum Ribbons

**V. N. Ageev, E. Yu. Afanas'eva, N. D. Potekhina, and A. Yu. Potekhin**

*Ioffe Physicotechnical Institute, Russian Academy of Sciences, Politekhnicheskaya ul. 26, St. Petersburg, 194021 Russia*

Received May 12, 1999

**Abstract**—The interaction of silicon with tantalum is studied by the Auger spectroscopy and temperature-controlled desorption technique. It is shown that, at a monolayer coating, the adsorbed silicon atoms penetrate into the bulk of a substrate at temperature $T \geq 1400$ K. The spectral shape and the annealing curves are explained by the influence of the Si–Si lateral repulsion in an adsorbed layer on the desorption and diffusion of the Si atoms into the bulk. Some ratios between the kinetic parameters are determined from analysis of the experimental data. Their application in numerical calculations based on the model proposed earlier makes it possible to determine (from comparison of the calculated and experimental data) the kinetic parameters for all the processes of the interaction between silicon and the tantalum substrate during the temperature-controlled desorption (desorption, transfer into the bulk, diffusion, and migration of silicon onto the surface). An adequate description of the experiment is obtained only under the assumption that the diffusion at the final stages of temperature-controlled desorption after reaching a maximum occurs within a thin layer near the surface, so that the migration of the Si atoms to the surface and desorption proceed more rapidly than their diffusion into the bulk. © *2000 MAIK "Nauka/Interperiodica".*

Although the refractory metal–silicon contacts are promising elements of high-temperature microelectronics, the processes of their formation have thus far been imperfectly understood. For this purpose, it is common practice to examine the system "a semiconductor coated with a metal layer" [1]. In studies performed in our laboratory, we have dealt with the systems "a metal covered with a semiconductor layer." This provides a means for revealing new aspects of the formation of near-the-surface layers in the region of the studied contact. The present work continuities a series of systematic investigations of the interaction between silicon and refractory metals (such as W, Ir, Nb, and Ta [2–8]) by the Auger electron spectroscopy and temperature-controlled desorption technique. The interaction of silicon with tantalum was investigated by the photoelectron spectroscopy in [9]. The diffusion of silicon into tantalum and the silicide formation were examined by the X-ray diffraction in [10].

In this work, we measured the spectra of temperature-controlled desorption, the Auger signals, and the total amount of silicon remaining in a tantalum substrate after the annealing of the tantalum ribbon coated with a monolayer of silicon. The experimental data were compared with the results of calculations of the model system described in [11, 12]. The model system accounts for the processes of penetrating adsorbed atoms into the bulk of metal, their diffusion in the bulk, and transfer onto the surface upon temperature-controlled desorption and annealing. A comparison of the model calculation and the experimental results makes it possible to determine the rate constants for all the processes observed in the system and to refine their physical meaning.

## 1. EXPERIMENTAL TECHNIQUE

The measurements were performed by the temperature-controlled desorption technique. The desorption products were identified using a time-of-flight mass spectrometer. The pressure of residual gases in the instrument was $10^{-10}$ Torr. An absorbent was a textured tantalum ribbon with the surface predominantly formed by the (100) face $0.01 \times 1.5 \times 30$ mm in size. The ribbon surface was arranged within view of an ion source of the mass spectrometer. The ribbon was cleaned from carbon according to the standard procedure by the annealing in an oxygen atmosphere followed by temperature-controlled heating.

Silicon was deposited from small bars $1 \times 1 \times 30$ mm in size. The silicon bars were mounted parallel to the tantalum ribbon and then were subjected to dc heating. The ribbon temperature was determined from the temperature dependence of the resistance. This dependence was calibrated with an optical micropyrometer. The tantalum ribbon was heated by a direct current. The ribbon temperature in the course of the "flash" changed linearly with time. The flux of Si atoms was recorded from the flow of $Si^+$ ions, to which corresponded a 28 line in the mass spectrometer. The flux of Si atoms onto the tantalum ribbon was calibrated by the "quartz balance" method.

The experiments were performed as follows. The tantalum ribbon was heated at a temperature of 2600 K for several seconds. Then, the temperature of ribbon

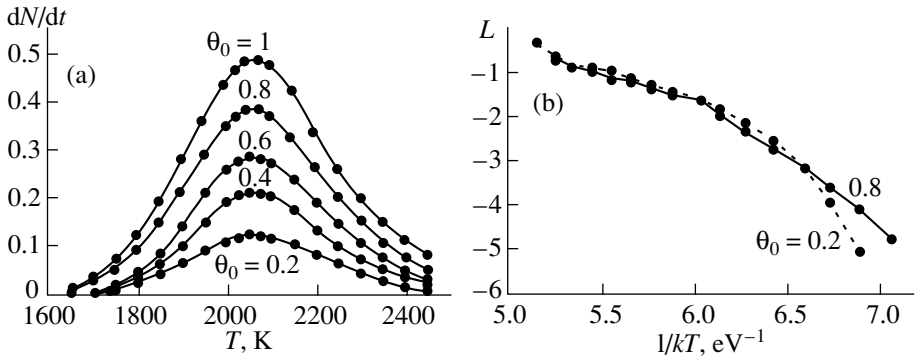


**Fig. 1.** (a) Experimental spectra of temperature-controlled Si/Ta desorption at the initial silicon coverage $\theta_0 = 0.2$, 0.4, 0.6, 0.8, and 1.0 and (b) dependences of the function $L = \ln(N^{-1}dN/dt)$ on $(kT)^{-1}$ at the coverage $\theta_0 = 0.2$ (dashed line) and 0.8 (solid line).

was decreased to room temperature, silicon was deposited over different time intervals, and the flash was carried out. The annealing of the film with a silicon monolayer applied at $T = 300$ K was carried out at several temperatures $T_i$ in the range 1300–1800 K for 1 min. Prior to measurements, we established that the silicon desorption on the opposite side of the ribbon was absent both in the course of the flash and upon annealing of the ribbon with a silicon layer applied only on one side.

## 2. RESULTS

Figure 1a demonstrates the spectra of temperature-controlled desorption at the heating rate $\beta = 200$ K s$^{-1}$ and different initial silicon coverages $\theta_0 \leq 1$ for the Ta(100) surface. It is seen that, for all the coverages $\theta_0$, the spectra contain only one maximum. The maximum location and the halfwidth remain unchanged as the $\theta_0$ value increases, which is characteristic of the monoatomic desorption without lateral interactions in an adsorbed layer and without diffusion of adsorbed species into the bulk. In this case, the temperature-controlled desorption is described by the Arrhenius equation with the first-order desorption. However, in our case, the dependence $L(1/kT) = \ln(N^{-1}dN/dt)$, for which the graphs at two $\theta_0$ values are depicted in Fig. 1b, cannot be approximated by the straight line and, hence, cannot be described by the Arrhenius equation. The slope of the initial rectilinear portions of these curves (at $T \lesssim 1800$ K, i.e., $1/kT \gtrsim 6.4$ eV$^{-1}$) decreases with an increase in the coverage from $E^* \simeq 5.4 \pm 0.2$ eV at $\theta_0 = 0.2$ to $E^* \simeq 3.5 \pm 0.2$ eV at $\theta_0 = 0.8$. At higher temperatures, the $L(1/kT)$ curves become less dependent on $\theta_0$, and their slopes decrease as the temperature increases up to 2200 K.

Since the spectra of temperature-controlled desorption at $\theta_0 \leq 1$ cannot be described by the Arrhenius equation with the first-order desorption, it would be reasonable to consider other processes for their explanation, such as, for example, the diffusion of silicon into the bulk of a tantalum ribbon upon temperature-controlled desorption. In order to verify the possibility of the diffusion process to occur, we studied the dependence of the intensity of the silicon Auger signal on the temperature $T_i$ of annealing a silicon monolayer film on the tantalum substrate. Figure 2 displays the annealing curves (dashed lines) drawn through the experimental points—the temperature dependence of the intensity of the Auger signal (curve *1*) and the dependence of the total amount of silicon remaining in the system after annealing (curve *2*). The solid line corresponds to the theoretical approximation discussed in Section 3.

The decrease in intensity of the Auger signal $I_A(T)$ (curve *1*), which is proportional to the silicon amount in near-the-surface layers, occurs with an increase in the $T_i$ temperature due to the silicon desorption during the annealing and also the diffusion of silicon into the bulk of tantalum. The total amount of silicon remaining in the system $M(T_i)$ decreases only through the desorption in the course of annealing and can be measured by the temperature-controlled desorption technique. Comparison of curves *1* and *2* in Fig. 2 shows that a decrease in the silicon amount in the near-the-surface region (at $T_i$

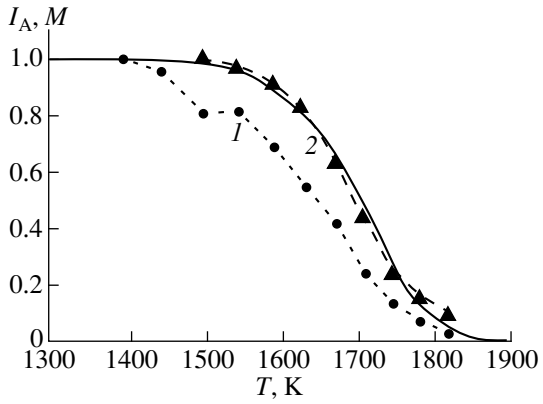


**Fig. 2.** Dependences of (*1*) the intensity of the Auger signal $I_A$ and (*2*) total amount of silicon $M(T)$ in a tantalum plate after annealing for 60 s on the annealing temperature.

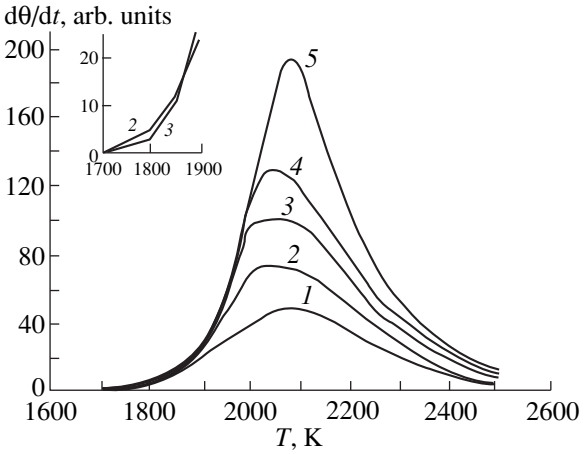


**Fig. 3.** Experimental spectra of temperature-controlled Si/Ta desorption at large silicon coverage $\theta_0$ = (*1*) 1.2, (*2*) 1.6, (*3*) 2.0, (*4*) 2.4, and (*5*) 3.2.

≥ 1400 K) occurs prior to the desorption and a decrease in M($T_i$) (at $T_i \geq 1500$ K). This implies that, in the range $1400 \leq T_i \leq 1500$ K, only the diffusion of silicon into the bulk of tantalum substrate takes place, and, at $T_i \geq$ 1500 K, the diffusion of silicon in the bulk is accompanied by its desorption from the surface of tantalum. Below $T_i \leq 1400$ K, the silicon monolayer on the tantalum surface remains stable in both processes.

Figure 3 shows the spectra of temperature-controlled desorption at large silicon coverages $\theta_0 > 1$. The initial portions of the spectra at $\theta_0 = 1.2$ and 1.6 (curves *1*, *2*) differ from those at $\theta_0 > 2$ (curves *3–5*). Upon further increase in the coverage, the edges of thermodesorption curves *3–5* coincide, and the maxima shift with an increase in $\theta_0$ toward the high-temperature range. This indicates the zero order of desorption, which is characteristic of the desorption from a thick layer of an adsorbate. Indeed, in this case, the dependence of $\ln(N^{-1}dN/dt)$ on $(kT)^{-1}$ is adequately reproduced by the straight line with the slope $E^* = 5.4 \pm 0.2$ eV. As is known [8], upon deposition of silicon on tantalum in the temperature range $1300 < T \leq 1600$ K at the initial coverages $\theta_0 < 2$, silicon is accumulated in near-the-surface region followed by formation of the $Ta_5Si_3$ silicide. In the case when the deposited silicon coverage becomes somewhat larger, i.e., $\theta_0 \simeq 2$, the structural phase transition from $Ta_5Si_3$ to $Ta_4Si$ is observed in near-the-surface region. Hence, the differences in the initial portions of the temperature-controlled desorption curves at $\theta_0 < 2$ and $\theta_0 > 2$ are likely accounted for by the desorption of silicon from different silicides, namely, $Ta_5Si_3$ and $Ta_4Si$. This process is accompanied by a drastic increase in the rate of dissolution of silicon through the silicide layer [8].

At $\theta_0 \geq 2$, the edges of the desorption curves coincide, and the maxima are shifted to the high-temperature range. The fact that the desorption rate does not depend on the coverage is likely due to the desorption of silicon from the $Ta_4Si$ silicide. The activation energy of desorption, which is found from the dependence $L(1/kT)$, coincides with the desorption energy at small coverages $\theta_0$, i.e., $E_d = 5.4 \pm 0.2$ eV, which indicates a small surface concentration of silicon atoms during the sublimation of silicide.

It should be noted that, if the temperature $T_{ads}$, at which silicon was deposited on tantalum, is less than 1300 K, the shape of the temperature-controlled desorption curves, unlike the silicon layer on the tungsten surface at $\theta_0 > 1$ [4], does not depend on $T_{ads}$ both at $\theta_0 \leq 1$ and $\theta_0 > 1$, even though the penetration of silicon into tantalum at $\theta_0 > 1$ occurs already at $T > 700$ K [8]. This means that the ultimate concentration profile of silicon in the bulk of tantalum is achieved during the flash.

## 3. COMPARISON OF EXPERIMENTAL RESULTS AND MODEL CALCULATIONS OF TEMPERATURE-CONTROLLED DESORPTION

As follows from the data shown in Figs. 1–3, the temperature-controlled desorption of Si atoms from the Ta(100) surface is accompanied by the penetration of silicon into the bulk of substrate, which occurs prior to the desorption from the adsorbed layer. A decrease in the slope of the initial portions of the $L(1/kT)$ curves in Fig. 1b with an increase in $\theta_0$ suggests a repulsive interaction between the adsorbed Si atoms on the Ta(100) surface, which is similar to the lateral Si–Si interaction on the W(100) surface [4].

Therefore, in order to describe the spectra of temperature-controlled desorption from submonolayer silicon films on the Ta(100) surface, it is necessary to take into account the diffusion of silicon into the bulk of substrate and its transfer onto the surface in the course of the flash, and also the lateral interaction in the adsorbed layer. The calculation of the model system for describing the spectra of temperature-controlled desorption under these conditions was performed in the earlier works [11, 12]. In these works, we dealt with a symmetric plate of thickness $2l$. Two surfaces of the plate were coated with a layer of an adsorbate at the initial coverage $\theta_0$. It was assumed that the diffusion and desorption proceed only at $T(t) \geq T_0$. At the initial instant, the volume is free from particles. In the model (Fig. 4), the first subsurface layer serves as a boundary of the remaining volume, which is treated as a continuum. The motion of particles in the continuum is characterized by the diffusion coefficient $D = D_0\exp(-E_m/kT)$. In [11], we described the set of equations for numerical solution to the problem of the concentration changes for particles in an adsorbed layer,

near-the-surface layer, and in the bulk upon temperature-controlled desorption at the condition

$$T(t) = T_0 + \beta t. \quad (1)$$

The temperature-controlled desorption was analyzed at different ratios between the rate constant of desorption $k_d$, the rate constant of transition from an adsorbed layer to near-the-surface layer $k_1$, the rate constant of transition from near-the-surface layer to the adsorbed layer $k_2$, and the diffusion coefficient $D(T)$.

An analogous problem was formulated more recently by Mavrikakis *et al.* [13], who considered the diffusion into the bulk in the course of deposition of an adsorbate. It was demonstrated that the more slowly proceeded the deposition, the higher the diffusion maximum was located in the spectrum in the high-temperature range. In our works, we assumed that the initial coverage has already been specified, and the influence of diffusion was studied only during the temperature-controlled desorption. However, unlike [13], we made allowance for the concentration changes in the subsurface layer at the boundary between the continuum and adsorbed layer [11] instead of the assumption on the quasi-stationary flow of particles at the boundary. One of the purposes of our earlier work [11] was to determine the conditions of forming the quasi-stationary flow at the boundary of continuum. It was shown that the quasi-stationary flow is formed only at the final stages of temperature-controlled desorption after reaching a maximum in the spectrum. Moreover, in [12], unlike [13], we also considered the influence of lateral interactions in an adsorbed layer on the spectra of temperature-controlled desorption.

In the absence of lateral interactions, the rate constants of all the processes follow the Arrhenius equation

$$k_i(T) = k_i^0 \exp(-E_i/kT), \quad (2)$$

where $k_i^0$ is the preexponential factor of the $i$th process, and $E_i$ is the activation energy of the $i$th process. The lateral interactions in the adsorbed layer result in the dependences of $k_d$ and $k_1$ on the coverage $\theta(t)$. We took this dependence from the lattice-gas theory [14, 15]. The spectrum of temperature-controlled desorption is determined by the flux of desorbable particles

$$J(t) = -dN/dt = N_s k_d(T(t))\theta(t), \quad (3)$$

(where $N(t) = N_s\theta(t)$ is the total number of particles in half the plate, and $N_s$ is the number of adsorption sites per 1 cm$^2$), and can contain one, two, and three maxima [11, 12]. In the presence of the lateral repulsion in an adsorbed layer, one maximum in the spectrum can be observed only when the repulsion affects both the desorption rate and the diffusion of particles into the bulk; in this case, the diffusion comes before the desorption.

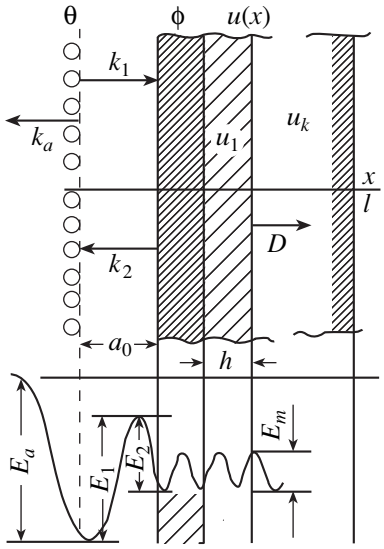


**Fig. 4.** A schematic model of the studied system.

In order to estimate the ranges of variations in the parameters involved in the calculation, we used the following findings.

(1) The slope of the dependence $L(1/kT) = \ln(N^{-1}dN/dt)$ (Fig. 1b) at small coverages $\theta_0 \longrightarrow 0$ determines the activation energy of desorption, that is,

$$E_d \simeq 5.4 \pm 0.2 \text{ eV}. \quad (4)$$

(2) The change in the slope of the $L(1/kT)$ curve with an increase in the coverage $\theta_0$ gives an estimate of the energy of lateral interaction $w$ from the relationship

$$E_i(\theta) \simeq E_i(0) - z\theta w, \quad (5)$$

where $z$ is the number of the nearest neighbors in an adsorbed layer, and $E_i = E_d$ or $E_1$.

The energy of the lateral interaction $w$ can be determined using the $E_d(0)$ value found from expression (4) and $E_d(1) \simeq 4.5$ eV. The latter value is taken to be close to the heat of sublimation of silicon, because the $E_d(1)$ energy obtained from the slope of the $L(1/kT)$ curve is not correct. This is explained by the fact that the temperature-controlled desorption occurs, as shown above, after the partial depletion of the adsorbed layer due to the diffusion of silicon into the bulk. In the case of desorption at the coverage $\theta_0 \simeq 1$, the lateral repulsion in the adsorbed layer should give rise to two maxima in the spectrum of temperature-controlled desorption [14, 15]. However, the spectrum of temperature-controlled Si/Ta desorption exhibits only one high-energy peak, which corresponds to small coverages. Hence, from formula (5) at $z = 4$, we obtain the estimate

$$w \simeq 0.25 \pm 0.05 \text{ eV}. \quad (6)$$

(3) The preexponential factors of the desorption process are evaluated from the location of the maximum in the spectrum of temperature-controlled desorp-

**Table 1.** Variants of the sets of parameters used in calculations

| | I | | II | | III | |
|---|---|---|---|---|---|---|
| | $E_i$ | $k_i^0$ | $E_i$ | $k_i^0$ | $E_i$ | $k_i^0$ |
| $k_d$ | 5.4 | 5 | 5.5 | 8 | 5.3 | 7 |
| $k_1$ | 4.6 | 1 | 4.7 | 1 | 4.4 | 5 |
| $k_2$ | 3.4 | 5 | 3.5 | 5 | 3.0 | 7 |
| $D$ | $2.1 \times 10^{-3}$ | | $1.8 \times 10^{-4}$ | | 1.6 | $2 \times 10^{-4}$ |
| $l_1$ | $0.15l$ | | $0.12l$ | | $0.25l$ | |

**Table 2.** Fraction of silicon in substrate after annealing for 60 s at different temperatures $T_i$ (experimental and calculated data correspond to sets of parameters I and III specified in Table 1)

| $T_i$, K | Experiment | I | | III |
|---|---|---|---|---|
| | | $l_1 = l$ | $l_1 = 0.15l$ | $l_1 = 0.25l$ |
| 1400 | 1.0 | 0.994 | 0.99 | 1.0 |
| 1500 | 1.0 | 0.988 | 0.98 | 0.98 |
| 1600 | 0.80–0.89 | 0.92 | 0.90 | 0.88 |
| 1700 | 0.38–0.46 | 0.72 | 0.60 | 0.52 |
| 1800 | 0.10 | 0.36 | 0.13 | 0.06 |

tion at $T_m \simeq 2060$ K according to the Redhead equation [16], which was derived without regard for diffusion into the bulk, that is,

$$E_d/(kT_m) \simeq \ln(k_d^0 T_m/\beta) - 3.64. \quad (7)$$

Here, the dependences $k_d(T)$ and $T(t)$ are found from equations (1) and (2).

(4) The temperature difference between the onset of the silicon diffusion into the tantalum substrate ($T_1$ = 1400 K) and the onset of desorption ($T_2$ = 1500 K) specifies the lower boundary for the difference of $E_d$ and $E_1$ according to the relationship $k_1(1400\ \text{K}) \simeq k_d(1500\ \text{K})$. By substituting formula (5) for the dependences of the activation energies $E_d$ and $E_1$ on the coverage into the Arrhenius equation (2) and taking into account the fact that, at $T_2$ = 1500 K, a certain part of the silicon coverage (about $0.1\theta_0$) passes into the bulk (Fig. 3), we obtain the expression

$$E_1 \simeq (E_d - 0.9\theta_0 zw)\frac{T_1}{T_2} + \theta_0 zw - kT_1 \ln(k_d^0/k_1^0). \quad (8)$$

From this formula at $k_d^0/k_1^0 \simeq (1\text{–}10)$, $w = 0.3$, $z = 4$, and $\theta_0 = 1$, it follows that

$$\delta E = E_d - E_1 \geq (0.4\text{–}0.8)\ \text{eV}. \quad (9)$$

(5) According to the theory of annealing a submonolayer in the presence of the diffusion into the bulk [17], the change in intensity of the Auger signal for impurity particles in the surface layer at the initial instants of annealing, i.e., at $t < k_d^{-1}(T)$, is determined by the relationships

$$I_A(t, T) \simeq I_0 \lambda \theta_0 [1 - b(T)\sqrt{t}],$$
$$b(T) = k_1(T)\sqrt{D}/[a_0 k_2(T)]. \quad (10)$$

Here, $a_0$ is the lattice constant for tantalum, and $\lambda$ is the penetration depth of the Auger signal for the impurity, which decays with an increase in its distance $x$ from the surface according to the law $I_A(x) = I_0 \exp(-x/\lambda)$, where $I_0$ is the intensity of the Auger signal from the monolayer. Comparison between the experimental data for the Si/Ta desorption [7] and expression (10) in [17] gives the following relationships

$$E_1 - E_2 \simeq (1.9 - E_m/2)\ \text{eV}; \quad k_2^0/k_1^0 \simeq 5, \quad (11)$$

where $E_2$ is the activation energy of the reverse transfer of particles from the bulk onto the surface, and $E_m$ is the activation energy of bulk migration.

Expressions (10) and (11) were derived without regard for the fact that the coefficients $k_d(\theta, T)$ and $k_1(\theta, T)$ depend on $\theta$. Hence, the estimates obtained from formulas (11) are tentative and can change with allowance made for these dependences.

(6) In the course of our experiment, no particle transfer to the opposite side of the ribbon 0.01 mm thick was observed. The distributions of particles throughout the bulk, which were calculated at different diffusion coefficients with the parameters meeting conditions (1)–(5), indicate that the silicon atoms do not reach the opposite side of the ribbon upon both annealing and temperature-controlled desorption, provided that the diffusion coefficient is limited by the inequality

$$D(T) \geq 10^{-4} \exp(-1.5\ \text{eV}/kT). \quad (12)$$

From the above considerations, we obtain a set of the initial parameters, which, after additional small variations, provide a more adequate description for the spectra of temperature-controlled desorption (Fig. 1) and the annealing curves (Fig. 2). The initial sets of kinetic parameters at different diffusion coefficients $D(T)$ are listed in Table 1 (variants I and II). The activation energies are given in eV, and the preexponential factors are expressed in units of $10^{13}$ s$^{-1}$ for $k_i^0$ and cm$^2$ s$^{-1}$ for $D_0$.

The calculations with these parameters for $l = 10^{-3}$ cm rather closely reproduce the main features of the spectrum, in particular, one maximum whose location and halfwidth virtually do not change with changes in the initial coverage $\theta_0$ (Fig. 5). However, unlike the experiment, the calculated spectrum appears to be asymmetric in shape, and the annealing rate at high temperatures is considerably less than the experimental value

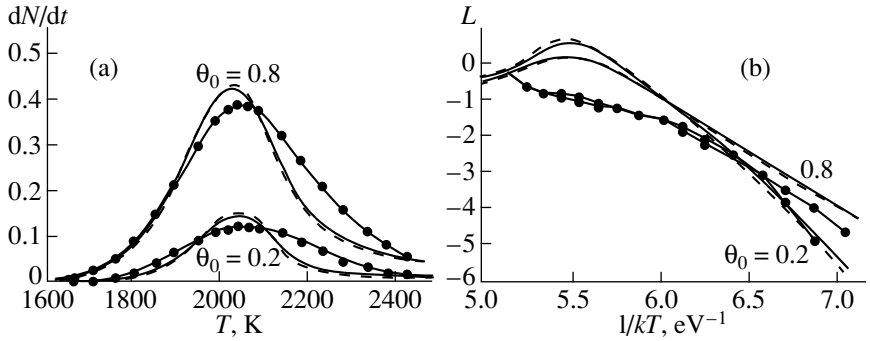


**Fig. 5.** Calculated (a) spectra of temperature-controlled desorption and (b) function $L(1/kT)$ at sets of parameters I (solid lines) and II (dashed lines) specified in Table 1 and $l_1 = l = 0.001$ cm. Points connected by solid lines represent the experimental data at the coverages (a) $\theta_0 = 0.2$, 0.6, and 1.0 and (b) $\theta_0 = 0.2$ and 0.8.

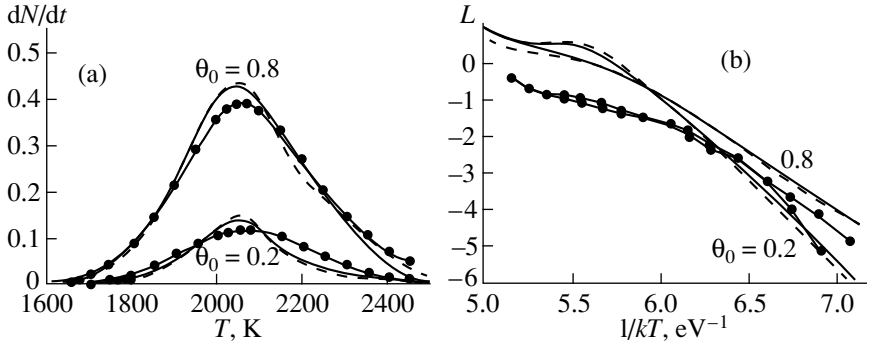


**Fig. 6.** The same data as in Fig. 5, but at $l_1 < l$ specified in Table 1.

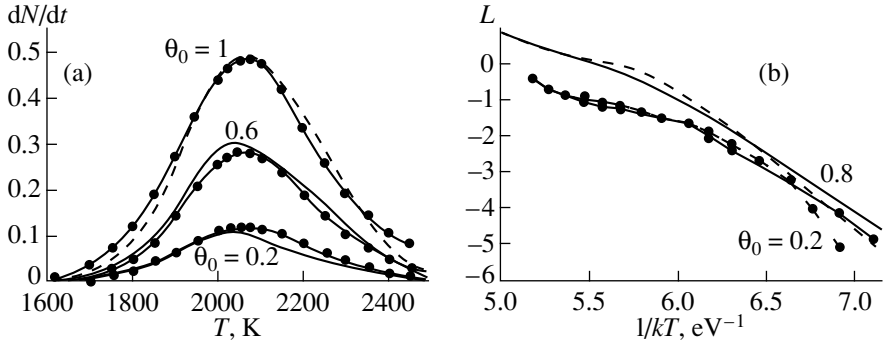


**Fig. 7.** Calculated (a) spectra of temperature-controlled desorption and (b) function $L(1/kT)$ at set of parameters III specified in Table 1. Points connected by solid lines represent the experimental data at the coverages (a) $\theta_0 = 0.2$, 0.6, and 1.0 and (b) $\theta_0 = 0.2$ and 0.8.

(Table 2, $l_1 = l$). This implies that the amount of silicon remaining in the bulk after the annealing at $T \geq 1700$ K is overestimated in the calculation more than three times irrespective of the diffusion coefficients satisfying condition (12). The additional variations mentioned above, which we produced in the found parameters, did not eliminate this discrepancy with the experimental data. The $L(1/kT)$ function (Fig. 5b) in the calculation ceases to increase and decreases at $T \geq T_m$, which, as was shown in [11, 12], also indicates an increased role of the silicon diffusion into the bulk in our model as compared to the experiment.

The symmetric shape of the calculated spectra can be obtained only by assuming that the diffusion rate drastically decreases in the bulk outside a certain layer with thickness $l_1 \ll l$ in the vicinity of the surface. With this assumption, all the variants specified in Table 1 give the symmetric shape of the spectra similar to those shown in Fig. 6, in which the calculated data were

obtained with the parameters of variants I and II at $l_1 < l$. The behavior of the $L(1/kT)$ function (Fig. 6b) also more closely resembles the behavior of the experimental curves. At high temperatures, the annealing proceeds more rapidly, and the discrepancy between the calculation and the experiment is almost absent, as it is seen from Table 2. Note that, in this variant of the theoretical model, restriction (12) becomes redundant.

A better fitting to the experimental data was achieved with a certain variation in the constants (variant III in Table 1) (Fig. 7). Deviations from conditions (11) in this set of parameters can result from the approximations made in [17] and also from the constraint between the parameters $E_i$ and $k_i^0$, which makes impossible their unambiguous determination separately from each other. The interrelation between the parameters provides a means for describing the experimental data by different sets of parameters. However, all the found sets only slightly differ from one another, and, in the case of the interaction between the silicon submonolayer and the tantalum substrate, the parameters are limited by the following ranges (the activation energies are given in eV, and the $k_i^0$ preexponential factors are expressed as $10^{13}$ s$^{-1}$):

$$E_d \simeq 5.3\text{–}5.5; \quad k_d^0 \simeq 5\text{–}10;$$
$$E_1 \simeq 4.4\text{–}4.7; \quad k_1^0 \simeq 1\text{–}8;$$
$$E_2 \simeq 3.0\text{–}3.5; \quad k_2^0 \simeq 3\text{–}7;$$
$$E_m \simeq 1.6\text{–}2.1; \quad D_0 \simeq 10^{-4}\text{–}10^{-3}\ \text{cm}^2\ \text{s}^{-1}. \qquad (13)$$

In our model, we assumed that the diffusion rate in the bulk of the plate decreases to zero outside the thin layer near the surface. For the actual system, this means that the diffusion rate of impurity particles in the bulk depends on their concentration or their distance from the surface. We simulated this dependence by the stepwise decrease in $D(T)$ down to zero at $x \geq l_1 = (0.12\text{–}0.25)l$, where $l$ is the thickness of the tantalum plate. The roughness of this model is partly responsible for the inexact description of the calculated dependences $dN/dt$ and $L(1/kT)$ at different coverages $\theta_0$. In particular, the stepwise decrease in the diffusion coefficient leads to a more drastic decay of the high-temperature branch of the spectrum as compared to the experiment. The shape of the experimental curve $L(1/kT)$ is more adequately described by the model with the stepwise dependence of the diffusion coefficient $D(x)$ as compared to the model without this assumption (Figs. 5, 6). The slopes of different portions of the $L(1/kT)$ curve (Fig. 7), which determine the effective activation energies $E_i$, are in reasonable agreement with the experiment. The remaining quantitative discrepancies can be accounted for by the inaccuracy of both the model and the measurements. The data on annealing, which were calculated with the proposed model (the last column in Table 2 and the solid line in Fig. 2), also agree well with the experiment.

The above calculations showed that a set of conditions (4)–(12) determines rather narrow ranges for variations in the parameters of rate constants specified by relationships (13).

Thus, it was demonstrated that, in the course of the temperature flash, silicon from the submonolayer penetrates into the bulk of substrate (at $T \geq 1400$ K) prior to its desorption (at $T \geq 1500$ K). This explains the presence of only one maximum in the spectrum of temperature-controlled desorption of silicon from the surface of tantalum, even with the lateral repulsion in the adsorbed layer.

From comparison of the calculated and experimental data, it follows that the experimental bell-shaped (almost without diffusion "tail") spectrum can be realized only when the diffusion rate is increased within a certain layer near the surface as compared to the rest of the system. This can be associated with the formation of a silicide layer at $T \geq 1600$ K, which provides the accelerated diffusion of silicon into the bulk and also a more rapid transfer of silicon to the surface through the layer of decomposing silicide in comparison with its penetration farther in the bulk of pure tantalum. Thus, the model with "reflection" of diffusing particles from the boundary of a certain layer near the surface better reproduces the spectrum of temperature-controlled desorption and the annealing rate than the model with a constant diffusion coefficient throughout the bulk of the ribbon.

The approximate values were determined for the activation energies and preexponential factors of the rate constants for all the processes of the interaction between adsorbed silicon atoms and the tantalum substrate.

## ACKNOWLEDGMENTS

This work was supported by the "Surface Atomic Structures" Program of the Ministry of Science and Technology of the Russian Federation, project no. 4.5.99.

## REFERENCES

1. G. Rossi, Surf. Sci. Rep. **7**, 1 (1987).
2. V. N. Ageev, E. Yu. Afanas'eva, N. R. Gall', *et al.*, Poverkhnost, No. 5, 7 (1987).
3. V. N. Ageev, E. Yu. Afanas'eva, N. R. Gall', *et al.*, Pis'ma Zh. Éksp. Teor. Fiz. **12** (9), 565 (1986).
4. V. N. Ageev and E. Yu. Afanas'eva, Poverkhnost, No. 7, 30 (1987).
5. E. Yu. Afanas'eva, N. D. Potekhina, and S. M. Solov'ev, Fiz. Tverd. Tela (S.-Peterburg) **37** (2), 463 (1995).
6. V. N. Ageev, E. Yu. Afanas'eva, S. M. Solov'ev, *et al.*, Fiz. Tverd. Tela (Leningrad) **35** (2), 481 (1993).

7. N. R. Gall, E. V. Rut'kov, A. Ya. Tontegode, *et al.*, Phys. Low-Dim. Struct. **4/5**, 75 (1996).
8. V. N. Ageev and E. Yu. Afanas'eva, Fiz. Tverd. Tela (S.-Peterburg) **39** (8), 1484 (1997).
9. T. A. Nguyen Tau, V. Azizan, and J. Derrien, Surf. Sci. **189/109**, 339 (1987).
10. G. J. Campisi, A. J. Bevolo, N. R. Shanks, *et al.*, J. Appl. Phys. **53**, 1714 (1982).
11. V. N. Ageev, A. Yu. Potekhin, and N. D. Potekhina, Poverkhnost, No. 1, 31 (1987).
12. V. N. Ageev, A. Yu. Potekhin, and N. D. Potekhina, Poverkhnost, No. 1, 5 (1991).
13. M. Mavrikakis, J. M. Schwank, and Y. L. Gland, Surf. Sci. **355**, 385 (1996).
14. D. L. Adams, Surf. Sci. **42**, 12 (1974).
15. V. P. Zhdanov, *Elementary Physical Chemical Processes on Solid Surfaces* (Plenum, New York, 1991).
16. P. A. Redhead, Vacuum **12** (2), 203 (1962).
17. N. D. Potekhina, Fiz. Tverd. Tela (S.-Peterburg) (1999) (in press).

*Translated by O. Borovik-Romanova*